0026-895X/92/050900-08$03.00/0

MOLECULAR PHARMACOLOGY, 41:900-907

Effects of Low Doses of Bicuculline on *N*-Methyl-D-aspartate Single-Channel Kinetics Are Not Evident in Whole-Cell Currents

JERRY M. WRIGHT[1] and LINDA M. NOWAK
Department of Pharmacology, Cornell University, Ithaca, New York 14853
Received March 15, 1991; Accepted February 25, 1992

SUMMARY

Bicuculline methiodide (BIC-MeI) (10–100 μM) altered the kinetics of *N*-methyl-D-aspartate (NMDA) responses in single-channel and whole-cell recordings. The principal effect of BIC-MeI (10–100 μM) on NMDA channels was a dose-dependent decrease in mean channel open time (τ_o), accompanied by the introduction of a new closed time (τ_B) of 14.0 ± 3.5 msec (mean ± standard deviation; $n = 14$) in closed time distributions, which was independent of BIC-MeI concentration. BIC-MeI (10–100 μM) increased the frequency of NMDA channel opening in a dose-dependent manner, offsetting the decrease in τ_o, such that the total time spent in the open state per minute was unchanged, and thus the total charge/min through NMDA channels was unchanged. Similarly, the amplitudes of NMDA whole-cell current responses were not noticeably affected by 10–80 μM BIC-MeI, even though power spectra density analysis of the whole-cell NMDA-stimulated noise revealed changes in the underlying channel kinetics in the presence of BIC-MeI. Taken together, the effects of 10–80 μM BIC-MeI on NMDA responses were consistent with the predictions of the sequential block model; however, the effects of BIC-MeI exhibited no obvious voltage dependence. In addition to the low-dose effects of BIC-MeI, 100 and 200 μM BIC-MeI inhibited whole-cell NMDA responses. The inhibition by 100 μM BIC-MeI was not large, but it was augmented from 15% to 30% by increasing the NMDA concentration from 10 μM NMDA to 20 μM NMDA, indicating that channel activation was necessary for BIC-MeI-mediated inhibition. Preliminary single-channel experiments performed under conditions conducive to trapping of an open channel blocker at its binding site indicated that the effect of BIC-MeI on τ_o persisted after the removal of the blocker, consistent with use dependence of the dissociation of BIC-MeI from the NMDA receptor-channel complex.

BIC, a naturally occurring plant alkaloid, is a competitive antagonist of $GABA_A$ receptors that increases neuronal excitability in brain by disinhibition (1, 2). A variety of derivative forms of BIC, with differing degrees of effectiveness as $GABA_A$ antagonists, are available (2). Although BIC is a more potent inhibitor of GABA responses than is BIC-MeI (2), the BIC form is unstable and rapidly undergoes temperature- and pH-dependent decomposition to bicucine (3). Thus, the antagonist effect of BIC on GABA responses declines rapidly in a 35° solution at pH 7.4 (4). In contrast, a solution of BIC-MeI is stable for at least 12 hr (2).

In an attempt to suppress a 35-pS Cl^- channel that coexisted with NMDA channels in some outside-out patches, we observed that 20 μM BIC-MeI decreased the mean open time of NMDA channels. Because BIC (0.25–100 μM) is frequently used to block $GABA_A$ responses, in a variety of *in vitro* preparations, during studies of excitatory amino acids (5–7) and because it is used to generate experimental seizures that have been shown to be partially reversed by NMDA antagonists (8), we further investigated the effects of BIC-MeI on NMDA channels. BIC-MeI effects were examined in whole-cell and single-channel recordings.

Materials and Methods

Recording conditions. Mouse forebrain neurons were prepared from 15–17-day-old fetuses, as described previously (11). Recordings were performed at 20–25° on neurons grown in culture for 4–23 days. Whole-cell and outside-out patch-clamp configurations were used (12).

Solutions. Borosilicate glass patch pipettes (3–7 MΩ; WPI TW-150) contained (in mM) 140 CsCl, 10 EGTA-K, 1 $CaCl_2$, and 10 HEPES-K (pH 7.2). After preliminary investigations of BIC effects on Cl^- channels, 70 mM cesium acetate was substituted for 70 mM CsCl, to eliminate the chloride currents that continued to contaminate some NMDA single-channel recordings.

Extracellular (bath) solutions contained (in mM) 150 NaCl, 2.8 KCl, 1.0 $CaCl_2$, 10 HEPES-Na (pH 7.2), and 300 nM tetrodotoxin. Levels of

This work was supported by National Institutes of Health Grant NS24467 to L.M.N.
[1] Present address: National Institute on Alcohol Abuse and Alcoholism, 12501 Washington Ave., Rockville, MD 20852.

ABBREVIATIONS: BIC, bicuculline; APV, D-(−)-2-amino-5-phosphonovaleric acid; BIC-MeI, bicuculline methiodide; EGTA, [ethylene-bis(oxyethylenenitrilo)]tetraacetic acid; GABA, γ-aminobutyric acid; HEPES, *N*-[2-hydroxyethyl]piperazine-*N*′-[2-ethanesulfonic acid]; NMDA, *N*-methyl-D-aspartate; TOT, total open time per minute of recording; TEA, tetraethylammonium; BIC-Cl, bicuculline chloride.

divalent cations known to affect NMDA channel τ_o (9, 13, 14) were measured by atomic adsorption spectroscopy, as described previously (15), and were found to be too low (0.8 μM Mg^{2+}, 0.1 μM Zn^{2+}, 0.2 μM Ni^{2+}, and 0.4 μM Co^{2+}) in the 100 μM BIC-MeI solution to account for any of the effects observed. Glycine (1 μM) was added to all agonist-containing extracellular solutions unless otherwise stated. NMDA (Cambridge Research Biochemical), glycine (Sigma), and BIC-MeI (Sigma) were prepared as stock solutions and frozen. To limit degradation, the BIC (Sigma) stock solution was prepared fresh in 0.2 N HCl and kept acidic until immediately before use. All drugs were diluted in the bath solution and applied by local perfusion in the vicinity of the patch pipette, through a large-bore Pasteur pipet. It took 5–10 sec for complete changes of drug solutions to occur at the pipet tip. Total bath solution was continually exchanged by slow perfusion (1–3 ml/m) of the 35-mm culture dish.

Data analysis. Currents were recorded using a List EPC-7 patch-clamp amplifier. Data were initially filtered through an eight-pole Bessel filter at 4 kHz and were permanently stored in digital form on video cassettes, using a pulse code modulator (PCM-1B, Medical Systems Inc., Greenvale, NY). All data for analysis were taken from stable steady state portions of the records. Records were reconverted to analog form, refiltered at a lower frequency (500 Hz to 1 kHz Butterworth for whole-cell noise data and 1–2 kHz Bessel for single channels), and digitally sampled at a rate 5 times the filter cutoff frequency, using a ISC-16 data acquisition board (RC-Electronics, Goleta, CA). The minimum detectable time interval, or system dead time, was $0.179/f_c$, where f_c is the final cutoff frequency produced by the cumulative effects of filters in a cascade; this value was used to determine missed event compensation in fitting exponents to dwell time histograms (16). Analysis was done on personal computers (AST Premium 286), using the Channel Analysis Programs (RC-Electronics, Goleta, CA). Total charge/min was calculated from amplitude density histograms standardized to 1 min of recording, such as shown in Figs. 3B and 4. Gaussian functions were fit, using the Simplex algorithm, to all the sampled points. Total charge/min was then determined by integrating the area under the fitted peaks. The analysis software and system-testing procedures have been described in detail (15).

Results

Effects of BIC-MeI on whole-cell responses. BIC-MeI (100 μM) application, together with 1 μM glycine, did not evoke any direct response in cells (n = 2), whereas NMDA plus glycine stimulated responses in these same recordings. The effects of 5–200 μM BIC-MeI on NMDA response amplitude and noise were examined in whole-cell recording experiments conducted over the range of +40 to −80 mV (seven cells; 13 trials). No changes were seen in the amplitudes of NMDA responses with coapplication of 5–40 μM BIC-MeI (n = 5). However, spectral analysis did indicate dose-dependent changes in the time constants (τ) underlying the noise. No effect on τ was observed with 5 μM BIC-MeI, a 15% reduction was seen with 20 μM BIC-MeI, and a 50% reduction was observed with 40 μM BIC-MeI (Fig. 1). With 100 μM BIC-MeI there was also a decrease in the whole-cell NMDA response amplitude (see below). All aspects of NMDA responses returned to normal within 4 min of flushing out the BIC-MeI.

Effects of BIC-MeI in single-channel recordings. Single-channel data from one patch exposed to 5 μM NMDA in the absence of BIC-MeI (Fig. 2, *left*) and in the presence of an intermediate concentration of BIC-MeI (40 μM) (Fig. 2, *right*) show key features of the effects of BIC-MeI on NMDA channels. NMDA channel openings appeared to be briefer in the presence of 40 μM BIC-MeI, and there was an increase in the frequency of openings in a given time interval, as illustrated by the raw data traces in Fig. 2A. The apparent lack of change in NMDA channel amplitude in the presence of BIC-MeI, depicted in Fig. 2A, was verified in amplitude/probability density histograms (Fig. 2B). However, 40 μM BIC-MeI had a pronounced effect on NMDA mean channel open time (τ_o), decreasing it from 7.2 msec in control to 3.8 msec (Fig. 2C). Thus, the 21% reduction in total charge/min (Fig. 2B) must be due to a reduction in TOT, a measure that is a function of the number of events/sec and τ_o. In the experiment on the patch illustrated in Fig. 2, the increase in frequency of events only partially compensated for the 47% decrease in τ_o. However, in four other patches exposed to 40 μM BIC-MeI, the increase in the frequency of events did compensate for the effect on τ_o, with the net result being that the mean value of TOT in control and 40 μM BIC-MeI-containing solutions was not different.

The relationship between the effects of BIC-MeI concentration on τ_o, frequency of events, and TOT is shown, for 19 patches, in Fig. 3. The decrease in τ_o was dose dependent, with an IC_{50} of 55 μM BIC-MeI predicted for the reduction in τ_o. The association rate (k_+), determined from the slope of $1/\tau_o$ versus BIC-MeI concentration, was 3.3×10^6 sec^{-1} mol^{-1} (19 patches; 24 trials). The BIC-MeI-mediated reduction in τ_o appeared to be voltage independent between −40 and −100 mV. At low and intermediate BIC-MeI concentrations, the decrease in τ_o was compensated for by the increase in event frequency, such that TOT was essentially unchanged (Fig. 3). For example, with 40 μM BIC-MeI, TOT was 0.93 ± 0.14 (mean ± standard deviation; n = 5), compared with the normalized control value (i.e., TOT = 1.0). With 80 μM BIC-MeI, TOT did not decline significantly either (0.8 ± 0.2; mean ± standard deviation; n = 4), because, despite the decrease of the normalized τ_o to 40% of the control value, the frequency of events increased by 1.7-fold.

Application of BIC-MeI in doses ranging from 10 to 100 μM introduced a new closed time of 14 ± 3.5 msec (n = 14), which in the closed time distributions is referred to as τ_B, to signify the time in the blocked state. Due to the long duration of τ_B, measurements of the length of bursts of brief openings that occurred during typical rapid channel blocking and unblocking were generally not reliable. That is to say, the burst from one channel tended to merge temporally with the bursts from other channels in the multichannel patches, compromising accurate measurements of burst duration. However, the finding that TOT did not change with 10–80 μM BIC-MeI suggested that the burst length must be increased by BIC-MeI.

Inhibition of NMDA responses with higher concentrations of BIC-MeI. No inhibition of the total charge through NMDA channels/60-sec interval was observed in patches exposed to 5–80 μM BIC-MeI, even though NMDA channel τ_o decreased markedly. This was undoubtedly due to the compensatory increase in the frequency of events. Consistent with the findings on single-channel currents, the amplitudes of whole-cell NMDA currents were unaffected by these levels of BIC-MeI. However, inhibition of NMDA responses in cells (n = 4) was observed in the presence of 100 and 200 μM BIC-MeI, and convincingly so under particular conditions. For example, in one whole-cell recording the response to 100 μM BIC-MeI plus 10 μM NMDA was 13% smaller than the response to 10 μM NMDA alone. Upon increasing the NMDA concentration to 20 μM NMDA, the inhibition by 100 μM BIC-MeI was 21% of the response to 20 μM NMDA alone in the same cell. Thus, increas-

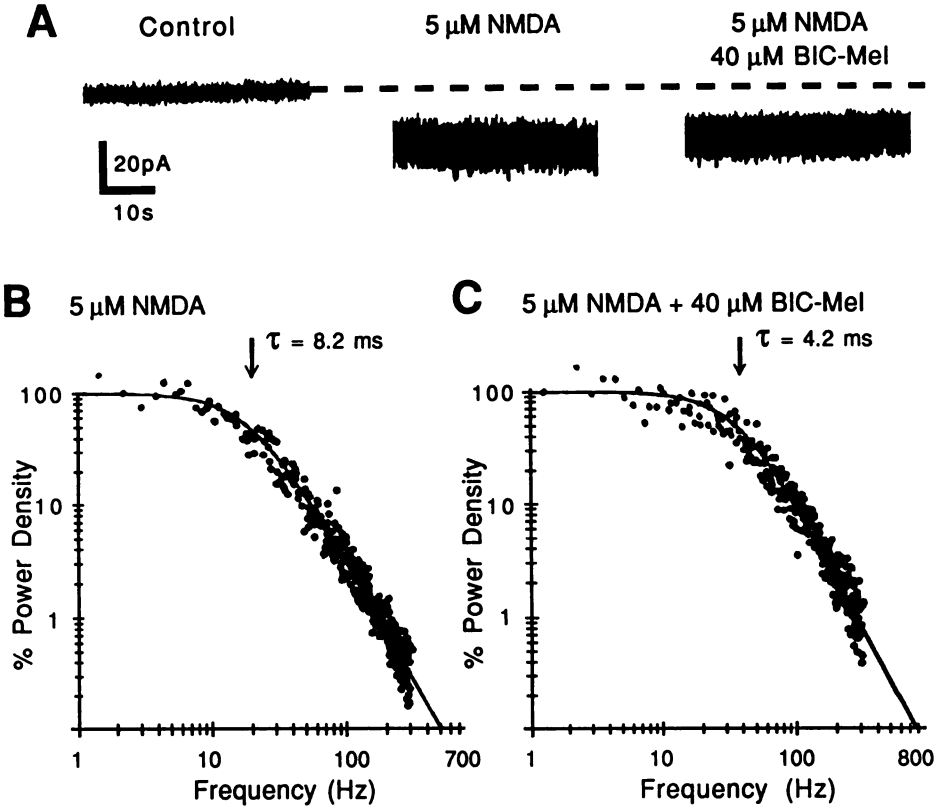

Fig. 1. Effects of BIC-Mel on whole-cell NMDA responses. A, DC current level and noise responses are shown for control (*left*), 5 μM NMDA (*center*), and 5 μM NMDA plus 40 μM BIC-Mel (*right*), with data placed to indicate the magnitude of the inward currents. *Dashed line*, control DC current. B, The power density spectrum for the control 5 μM NMDA response was fitted by a single Lorentzian function, with the time constant underlying the noise of $\tau = 8.2$ msec. C, With 40 μM BIC-Mel, the noise spectra were fitted by a single Lorentzian Function with $\tau = 4.2$ msec. Data were obtained at −60 mV at room temperature. Glycine (1 μM) was present in the agonist-containing solutions. Background noise spectra were subtracted in B and C. Data were filtered and sampled as described in Materials and Methods.

ing the agonist concentration increased the amount of inhibition by 100 μM BIC-MeI, suggesting that channel activation may influence BIC-MeI-mediated inhibition.

On the single-channel level, inhibition of responses to 5–10 μM NMDA by 100 μM BIC-MeI was generally small and unreliable; the decrease in the normal τ_o was large and it was not consistently compensated for by the associated increase in the frequency of events. As shown in Fig. 3B, the increase in the frequency of opening recorded with 10 μM NMDA plus 100 μM BIC-MeI was highly variable. In this particular condition, the normalized single-channel event frequency increased 2.1 ± 1.2 (mean ± standard deviation; $n = 7$). Nor was the inhibition significant with 100 μM BIC-MeI plus 10 μM NMDA, as reflected in the normalized TOT values, where TOT = 0.83 ± 0.3 ($n = 7$) (Fig. 3).

However, at higher NMDA concentrations inhibition by 100 μM BIC-MeI was observed consistently in patches (Fig. 4). Inhibition was observed in patches ($n = 4$; eight trials) exposed to 100 μM BIC-MeI plus 20 μM NMDA, where there was a 34.5 ± 11.7% decrease in the total charge/min. The total charge measure was used to quantify the data obtained with 20 μM NMDA, because it was not possible to determine the number of events or τ_o accurately at higher NMDA concentrations in patches that contained more than three levels of channel openings. Thus, at higher BIC-MeI concentrations, NMDA responses were inhibited by an uncompetitive mechanism, because inhibition was linked to channel activation.

Trapping of BIC-MeI. It was not possible to investigate the time course of the BIC-MeI inhibition and disinhibition because of the relatively slow drug application technique utilized in these experiments. However, given the observation that BIC-MeI-mediated effects required 2–3 min of perfusion with control solutions for complete reversal to occur, experiments designed to trap BIC-MeI at its binding site were attempted in excised patches. Thus, in single-channel studies, the question of use dependence of the BIC-MeI dissociation was addressed as follows. NMDA channels were 1) activated by exposure to 10 μM NDMA, 2) blocked with 80 μM BIC-MeI, and 3) treated with 100 μM APV in the continued presence of BIC-MeI and NMDA, to inhibit channel opening. The recording chamber was then flushed for 3–4 min with a bath solution containing 100 μM APV, to prevent the channels from opening while free BIC-MeI and NMDA were removed from the recording chamber. NMDA (10 μM) was then reapplied to the patch, without APV or BIC-MeI present, and the events occurring during successive 30-sec intervals were measured to determine τ_o. If BIC-MeI was trapped at a binding site on activated NMDA channels by channel closing using APV, the openings occurring after the second NMDA challenge (after the blocking and trapping sequence) should be shorter. This supposes that the NMDA receptor channel must be reactivated in order to permit BIC-MeI to dissociate from its binding site.

The complete experiment was carried out in two outside-out patches. In one patch, the steady state τ_o for 20 μM NMDA was 6.1 msec before BIC-MeI addition. At equilibrium in the presence of 80 μM BIC-MeI and 20 μM NMDA, τ_o was 2.0 msec. After the sequence of solution changes that would lead to trapping, reapplication of 20 μM NMDA produced 130 events in the first 30-sec interval, with τ_o of 3.0 msec, compared with the control τ_o of 6.1 msec (210 events) for the 30-sec period immediately after the first application of NMDA. τ_o recoveeed to 6.4 msec after 5 min of continuous NMDA application in the absence of BIC-MeI. Similar results were obtained from a second patch, with the control NMDA response having a τ_o of 5.9 msec during the first 30-sec interval of the first NMDA application (266 events), τ_o of 2.6 msec at equilibrium in 80 μM

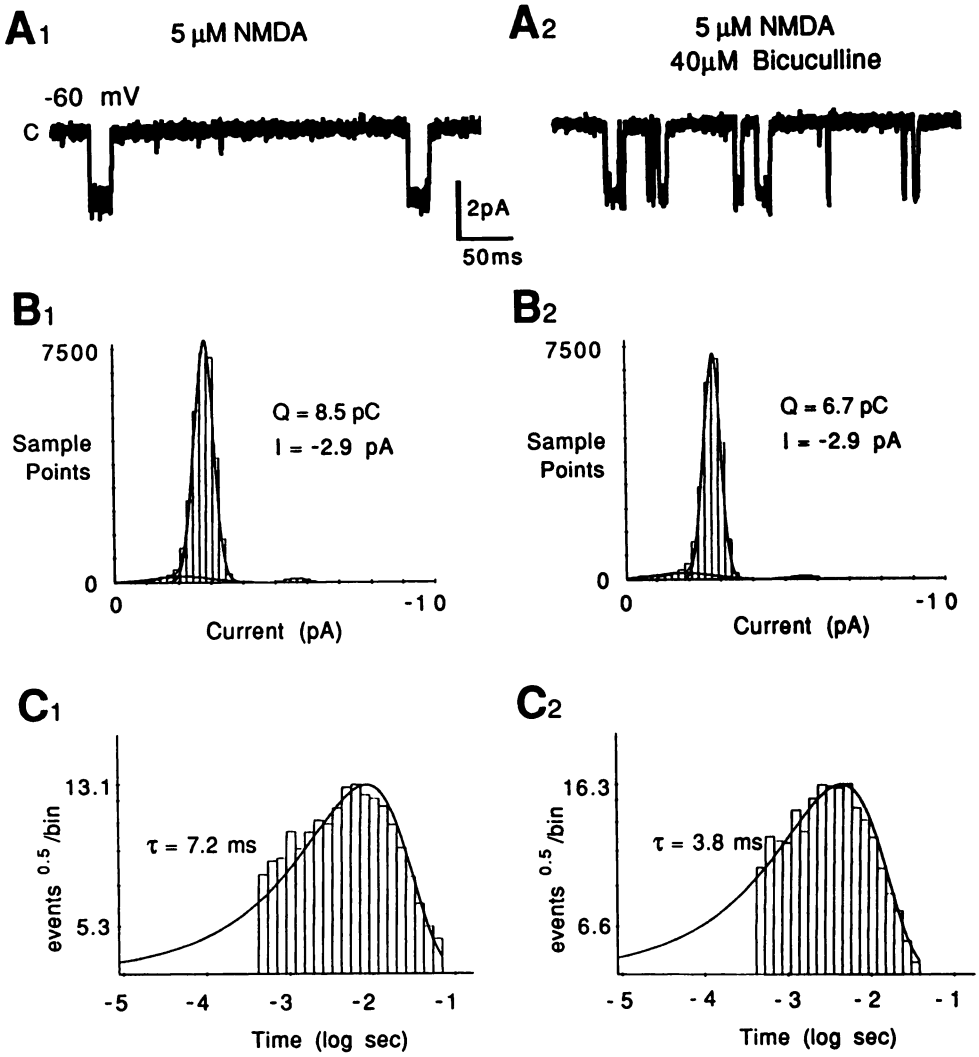

Fig. 2. Effects of 40 μM BIC-MeI at −60 mV are shown on a single-channel recording of NMDA-activated currents. A, Frequency of events increased, but there was little noticeable change in short data segments. The frequency of events was 7.1 events/sec for the 276-sec record with 5 μM NMDA (A_1) and 10.2 events/sec for the 285-sec record analyzed after the addition of 40 μM BIC-MeI (A_2). B, Amplitude/probability density histograms indicated a 21% reduction in total charge/min, from 8.5 pC/min (B_1) to 6.7 pC/min (B_2). Channel amplitude (−2.9 pA) was unchanged by 40 μM BIC-MeI. C, BIC-MeI reduced τ_o by 57%, from 7.2 msec (n = 1855 events) to 3.8 msec (n = 2905 events). The minimum detectable time interval was 0.5 msec. The patch pipette contained 4 mM Mg-ATP.

BIC-MeI plus NMDA, and τ_o of 3.6 msec (341 events) during the initial 30-sec interval of NMDA reapplication after the trapping protocol sequence. In this patch, τ_o recovered to 5.8 msec after several minutes of exposure to NMDA.

Apparent voltage independence of BIC-MeI inhibition. BIC-MeI-mediated inhibition appeared to be voltage independent in whole-cell recordings (compare Fig. 1 with Fig. 5) over the range of −60 to +40 mV. The increase in inhibition that was observed upon increasing of the NMDA concentration, at a given concentration of BIC-MeI, also occurred at both negative and positive potentials in cells.

The voltage independence of BIC-MeI effects was examined briefly in a small number of single-channel recordings. However, the experiment is difficult at positive potentials, because identification of NMDA channels is sometimes rendered ambiguous by the coexistence of Cl^- channels in the patches. Because the flow of Cl^- into the pipette evokes an outward current and Cl^- influx is not impeded by loading pipettes with larger impermeant anions such as acetate, currents through Cl^- channels can still interfere with interpretation of data acquired at positive potentials. The problem is actually exacerbated at positive potentials if the pipettes contain a 1:1 acetate/chloride mixture, because, by decreasing the internal Cl^-, the chloride equilibrium potential (E_{Cl}) is shifted to −19 mV, leading to an increase in Cl^- channel current amplitude at positive potentials. In two trials on one patch that did not contain spontaneously opening Cl^- channels, application of 80 μM BIC-MeI at +50 and +70 mV decreased τ_o by 47% and 27%, respectively. In another patch recorded at +30 mV, τ_o was reduced by 50% in 100 μM BIC-MeI, but analysis of the low amplitude openings at this potential required filtering the data at 500 Hz, thus reducing the relative precision of this τ_o measurement.

Lack of alteration by glycine of the BIC-MeI-mediated decrease in τ_o. Data from cells and patches indicated that BIC-MeI is not a competitive antagonist. Because the glycine site also plays a role in NMDA channel gating (17, 18), glycine concentration was manipulated in experiments conducted on four patches in the absence and presence of BIC-MeI. Increasing glycine from 1 to 10 μM in the presence of 40 μM (n = 2) or 80 μM BIC-MeI (n = 2) did not change the BIC-MeI-mediated decrease in τ_o. Thus, it is clear that the effect of BIC-MeI on τ_o is not due to actions at the glycine site.

BIC analogs. Effects of two other forms of BIC, BIC-Cl and bicucine, a breakdown product of BIC-Cl that accumulates slowly in solutions at pH ~7.0, were examined briefly, in order to determine whether these compounds would have effects on

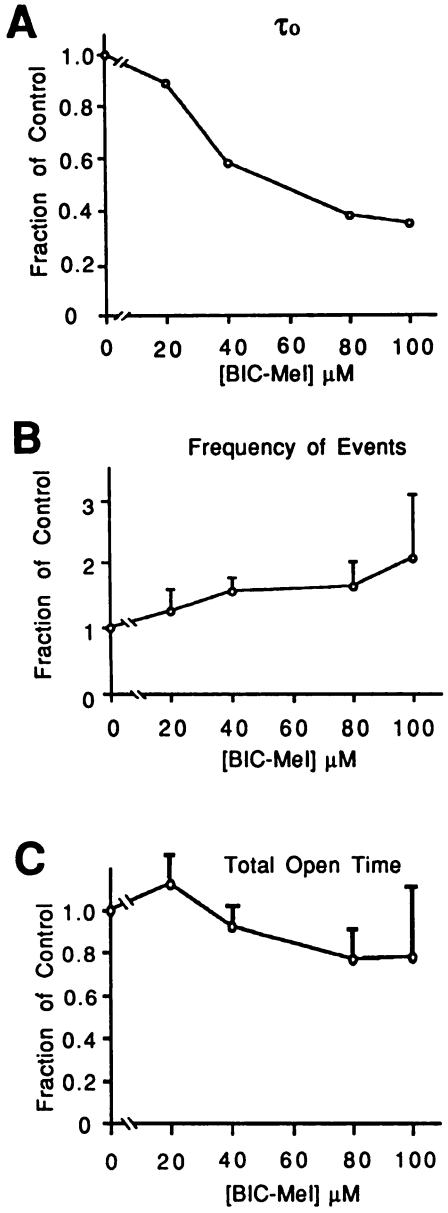

Fig. 3. Summary of single-channel responses to application of BIC-Mel. Data are from 19 outside-out patches where frequency of events and τ_o could be reliably measured in both control and test conditions; holding potentials were −40 to −100 mV. A, With 100 μM BIC-Mel, the NMDA channel τ_o was reduced to 35% of the normalized control values. Standard deviations of the measurements were within the points. B, The frequency of events increased with BIC-Mel concentration, and there was a 2.1-fold increase at 100 μM BIC-Mel. Frequency of events was normalized to control values for each patch. *Error bars*, standard deviation. C, A small (17%) but statistically insignificant decrease of TOT was observed with 100 μM BIC-Mel and 10 μM NMDA, which may account for current reductions seen in whole-cell recordings.

NMDA responses. NMDA channels in two patches exposed to 50 μM BIC-Cl and to 100 μM BIC-MeI both manifested the effects of BIC-MeI; τ_o decreased, frequency of opening increased, and TOT was unchanged. In one patch, τ_o was reduced from 5.4 to 4.1 msec in 50 μM BIC-Cl and the frequency of events increased 1.4-fold. Thus, at 1.1 times the control value, TOT was essentially unaffected by BIC-Cl. The recording chamber was then flushed with the NMDA solution before 100 μM BIC-MeI was applied. In the presence of BIC-MeI, NMDA

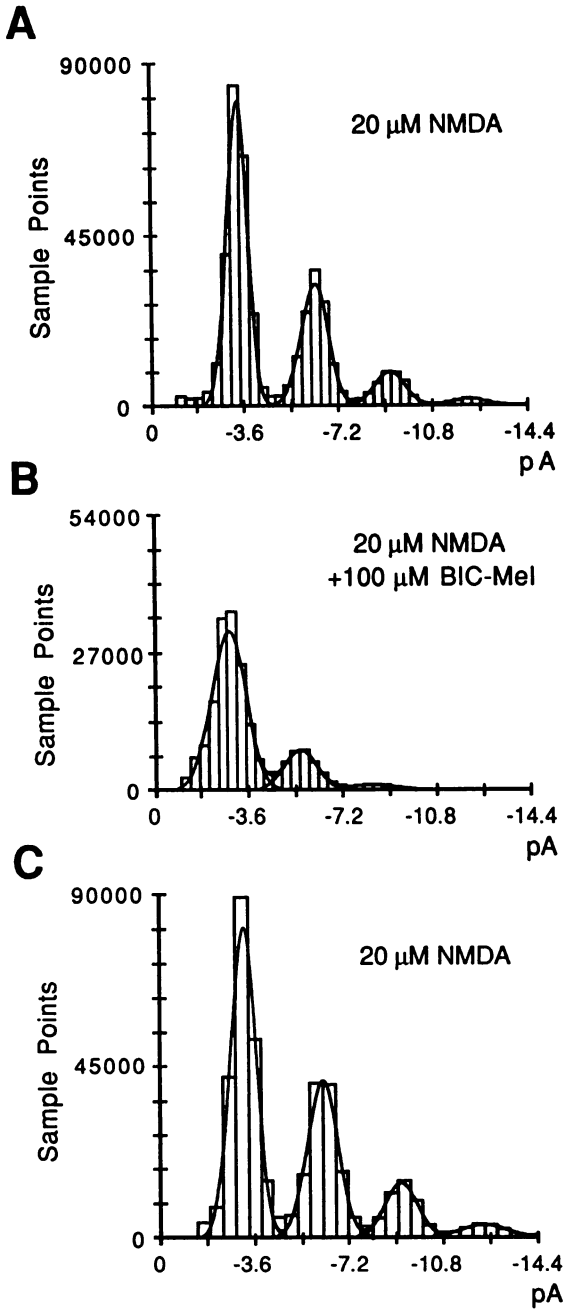

Fig. 4. Inhibitory effects of 100 μM BIC-MeI were apparent in patches exposed to 20 μM NMDA. A, The amplitude/probability density histogram of the response to 20 μM NMDA gave four peaks fitted by Gaussian functions. The current amplitude values were −3.6, −6.5, −9.2, and −12.2 pA, and the total charge/min through the NMDA channels in this patch was 205.6 pC. B, In the presence of 100 μM BIC-MeI plus 20 μM NMDA, three peaks were fitted by Gaussian functions. The current amplitude values were −3.1, −5.8, and −8.4 pA, and the total charge/min through the patch was 95.4 pC. C, After removal of the BIC-MeI, the response to 20 μM NMDA recovered. Four peaks were fitted by Gaussian functions, representing current amplitudes of −3.6, −6.5, −9.4, and −12.5 pA. The total charge/min was 214.8 pC. The small decreases in amplitude values with BIC-MeI are <1 SD of the Gaussian functions fitting the data. All solutions contained 1 μM glycine. Data were filtered at 2 kHz (Bessel) and sampled at 10 kHz. Histograms were originally constructed from 60 to 80 sec of record and standardized to represent 60 sec, as described previously (15).

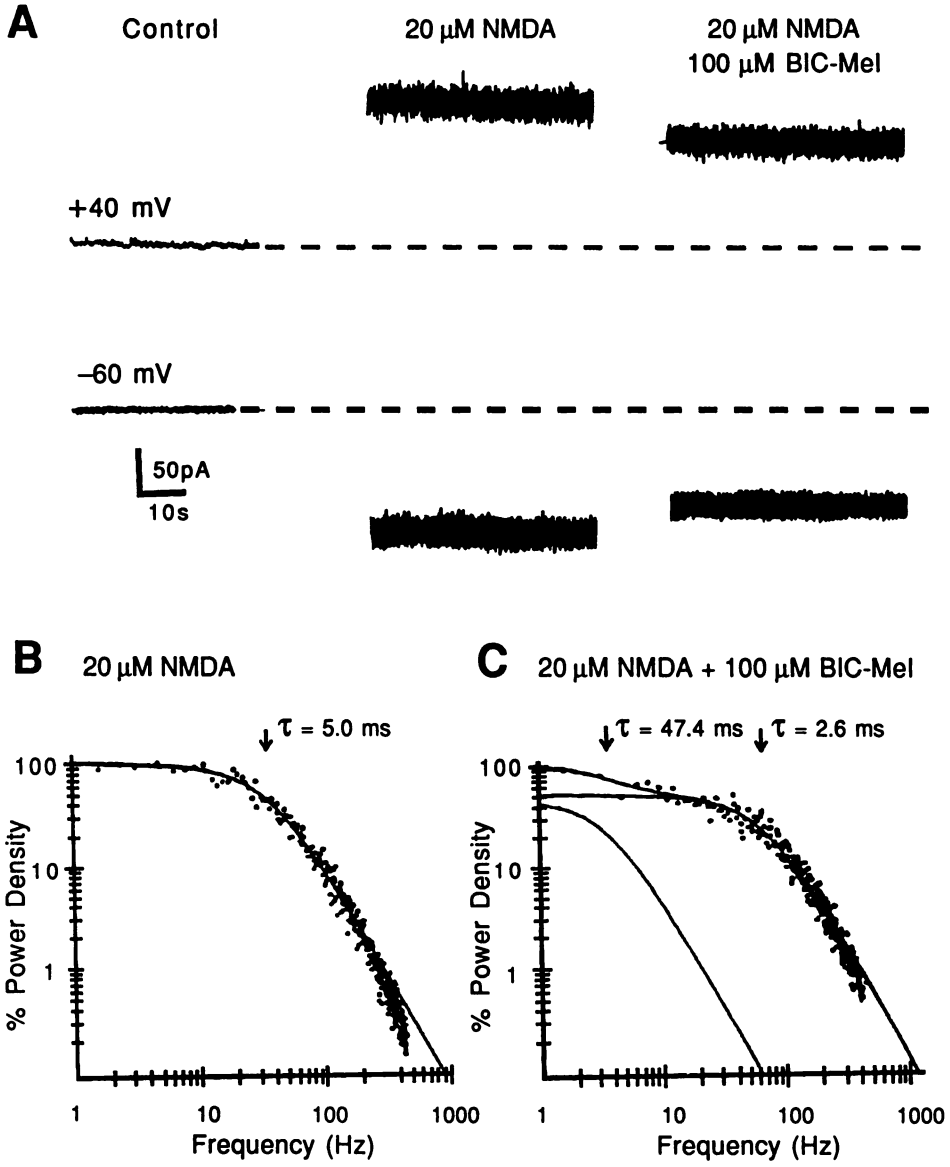

Fig. 5. Inhibitory effects of 100 μM BIC-MeI were voltage independent in whole-cell recordings. A, DC current level and noise responses are shown for control (*left*), 20 μM NMDA (*center*), and 20 μM NMDA plus 100 μM BIC-MeI (*right*), with data placed to indicate the magnitude of the currents. At +40 mV the response to 20 μM NMDA was decreased 29%, from +155 pA to +110 pA, by 100 μM BIC-MeI. At −60 mV the total current was reduced by 26%, from −135 pA to −100 pA. *Dashed lines*, control DC current level. B, The power density spectrum for the control 20 μM NMDA response at −60 mV was fitted by a single Lorentzian function, with the time constant underlying the noise of τ = 5.0 msec. C, With 100 μM BIC-MeI, the noise spectra changed substantially and were fitted by the sum of two Lorentzian components, with τ_1 = 47.4 msec and τ_2 = 2.6 msec. Glycine (1 μM) was present in the agonist-containing solutions. Background noise spectra were subtracted in B and C. Data were filtered at 1.0 kHz (Butterworth) and digitally sampled at 5 kHz.

τ_o decreased from 5.4 to 2.5 msec and, again, TOT was 1.1 times control. Repeating the experiment on another patch yielded similar results for 50 μM BIC-Cl, with a 29% decrease in τ_o and no change in TOT.

Because both synaptic and nonsynaptic BIC-Cl effects have been clearly demonstrated to decline rapidly at physiological pH, as BIC-Cl decomposes to bicucine (2, 4), the solutions from the BIC-Cl experiment previously described were allowed to stand at room temperature for 90 min before they were used on another patch to test the effects of increasing levels of bicucine in the solutions. Application of the BIC-Cl bicucine mixture decreased τ_o by 30% (from 6.4 to 4.5 msec), whereas TOT was unchanged. When 100 μM BIC-MeI was applied to the same patch, τ_o decreased to 2.1 msec and TOT was 1.2 times the control value.

In summary, the reductions in τ_o for both 50 μM BIC-Cl and the BIC-Cl bicucine mixture were less (25–30%) than the effect observed with 100 μM BIC-MeI (54–67%) on the same patches. The dose of BIC-MeI that decreased τ_o by 50% was 55 μM (n = 19 patches) (Fig. 3). Thus, the general effects of the BIC analogs were similar; BIC-Cl was not more potent than BIC-MeI and the effect of the BIC-Cl/bicucine mixture did not decrease with time, as would occur if bicucine were ineffective. Thus, there is no indication that the site of BIC interaction on NMDA receptor channels shares the $GABA_A$ receptor pharmacology, where the antagonist effectiveness is summarized as BIC-Cl > BIC-MeI > > bicucine.

Discussion

At lower doses of BIC-MeI, which decrease the τ_o and increase the frequency of channel openings, the absence of any change in TOT is consistent with the sequential model of open channel block. This model predicts that the number of openings per burst will increase and completely compensate for the reduction in τ_o (19, 20). This occurs because the model requires the blocking molecule to leave its binding site before the channel can enter the closed state. The model, as elaborated by Neher and Steinbach (20), predicted that the association rate ($1/\tau_o$) should be dependent on the blocker concentration but the dissociation rate ($1/\tau_B$) should be concentration dependent.

Both of these conditions are met by using 10–80 μM BIC-MeI. The important prediction of the sequential model is that in the presence of antagonist the bursts of brief openings will contribute the same amount of current as the opening of the channels in the unblocked state. In this regard, BIC-Cl, bicucine, and BIC-MeI at low doses all fit the sequential model, because TOT did not change, and no change in the amplitude of whole-cell NMDA responses was observed at the lower doses of BIC-MeI. Unfortunately, it was not possible to measure the increase in burst duration in our single-channel experiments, due to the presence of multiple channels in the patches. Indications of bursting were observed in power density spectra of whole-cell responses in the presence of higher doses of BIC-MeI (100–200 μM), which required spectra to be fitted by the sum of two Lorentzian functions.

In 1983, Neher (21) observed that, at high drug concentrations, block of nicotinic cholinergic channels by the anesthetic QX-222 decreased the total current per burst and, thus, the actions of this drug at high doses could not be described by the simple sequential model proposed previously for this drug at lower concentrations (20). Possible mechanisms suggested to account for the failure of the sequential model under these conditions were as follows: 1) the blocked channel might close, thereby reducing the charge per burst, 2) there may be a slow transition to a desensitized state, or 3) there may be a second slow channel block at higher doses. A second time constant within the interburst closed time distributions in the higher QX-222 concentrations favors hypothesis 3, but hypothesis 2 could not be ruled out. In single-channel recordings of block by 100 μM BIC-MeI, no second closed time was observed in closed time distributions; however, the study is inconclusive on this point, because a second closed state may be longer than the burst interval or because an insufficient number of longer closings may have been sampled.

For uncompetitive antagonists, which require receptor activation before inhibition can occur, increasing agonist concentration in the presence of the antagonist causes a greater degree of inhibition (22). In contrast, other forms of inhibition are at least partially overcome by increasing agonist concentration when the antagonist concentration is low (23). At the whole-cell level, the uncompetitive nature of BIC-MeI at high concentrations was clear, by these criteria.

It may be that BIC-MeI acts at a second site on the NMDA receptor channel to produce the uncompetitive antagonism observed. A voltage-independent decrease in the frequency of events/bursts has been observed with Zn^{2+} (9) and TEA^+ (15), leading to the suggestion that channel gating may be regulated by an allosteric site on the NMDA receptor-channel complex. The observed BIC-MeI inhibition of NMDA responses cannot be due to contamination by either substance, because TEA was not used in the experiments and the concentration of Zn^{2+} in the 100 μM BIC-MeI solution was 100 nM, which is substantially less than the 10 μM needed to observe such an effect on NMDA channels (9).

BIC-MeI actions did not exhibit any measurable voltage dependence. Although voltage-independent sequential block by uncharged compounds has been demonstrated (19, 24), and it is possible for both charged and uncharged compounds to interact with a binding site within a channel (25), lack of voltage dependence suggests that BIC-MeI is not sensitive to the transmembrane field and does not enter deeply into the pore to interact with any of the previously described binding sites (for review, see Ref. 26). However, the uncompetitive action of BIC-MeI suggests that the channel must open for the binding site to be accessible, and results of the trapping experiments suggest that BIC-MeI dissociation may be use dependent. Generally, the voltage independence of the BIC-MeI effects indicates that the drug may bind at a superficial location on the NMDA receptor-channel complex. Thus, the site or sites of regulation may be near the channel pore or located in a position where binding may interfere with channel gating. If so, it is possible that no effect would be seen unless the channel were opening and closing, as stimulated by the presence of agonist.

From a practical standpoint, the effects of BIC are likely to interfere with the interpretation of NMDA-induced responses in a number of situations. For example, during iontophoretic applications, local concentrations of BIC-MeI could easily exceed 100 μM. In such cases, care must be taken to determine whether BIC-MeI antagonism of NMDA responses may be contributing to the observed effects. In our experiments, >10 μM BIC-MeI was required to suppress adequately interference from Cl^- channels, but at this dose a decrease in NMDA channel τ_o was already apparent. Thus, the influence of lower doses of BIC-MeI on the kinetic rates of open NMDA channel blockers must be taken into account, because BIC compounds may block the pore or alter NMDA channel gating. By either mechanism, the K_d values of open channel blockers (e.g., Mg^{2+}, phenyclidine, ketamine, and MK-801) will be changed.

Acknowledgments

We thank Valerie Engle and Cornelia Poulopoulou for cell cultures and Paul Kline for writing the analysis software.

References

1. Curtis, D. R., A. W. Duggan, D. Felix, and G. A. R. Johnston. GABA, bicuculline and central inhibition. *Nature (Lond.)* **226**:1222–1224 (1970).
2. Olsen, R. W., M. Ban, and T. Miller. Studies on the neuropharmacological activity of bicuculline and related compounds. *Brain Res.* **102**:283–299 (1976).
3. Olsen, R. W., M. Ban, T. Miller, and G. A. R. Johnston. Chemical instability of the GABA antagonist bicuculline under physiological conditions. *Brain Res.* **98**:383–387 (1975).
4. Heyer, E. J., L. M. Nowak, and R. L. Macdonald. Bicuculline: a convulsant with synaptic and nonsynaptic actions. *Neurology* **31**:1381–1390 (1981).
5. Artola, A., and W. Singer. Long-term potentiation and NMDA receptors in rat visual cortex. *Nature (Lond.)* **330**:649–652 (1987).
6. Herron, C. E., R. Williamson, and G. L. Collingridge. A selective *N*-methyl-D-aspartate antagonist depresses epileptiform activity in rat hippocampal slices. *Neurosci. Lett.* **61**:255–260 (1985).
7. Dingledine, R., M. A. Hynes, and G. L. King. Involvement of *N*-methyl-D-aspartate receptors in epileptiform bursting in the rat hippocampal slice. *J. Physiol. (Lond.)* **380**:175–189 (1986).
8. Horne, A. L., N. L. Harrison, J. P. Turner, and M. A. Simmonds. Spontaneous paroxysmal activity induced by zero magnesium and bicuculline: suppression by NMDA antagonists and GABA mimetics. *Eur. J. Pharmacol.* **122**:231–238 (1986).
9. Christine, C. W., and D. W. Choi. Effect of zinc on NMDA receptor-mediated channel currents in cortical neurons. *J. Neurosci.* **10**:108–116 (1990).
10. Wright, J. M., and L. M. Nowak. Multiple effects of tetraethylammonium (TEA) on *N*-methyl-D-aspartate receptor-channels in cultured mammalian neurons. *Soc. Neurosci. Abstr.* **16**:85 (1990).
11. Ascher, P., P. Bregestovski, and L. Nowak. *N*-Methyl-D-aspartate-activated channels of mouse central neurons in magnesium-free solutions. *J. Physiol. (Lond.)* **399**:207–226 (1988).
12. Hamill, O. P., A. Marty, E. Neher, B. Sakmann, and F. J. Sigworth. Improved patch-clamp techniques for high-resolution current recording from cells and cell-free membrane patches. *Pflügers Arch.* **391**:85–100 (1981).
13. Mayer, M. L., and G. L. Westbrook. Permeation and block of *N*-methyl-D-aspartic acid receptor channels by divalent cations in mouse cultured central neurones. *J. Physiol. (Lond.)* **394**:425–427 (1987).
14. Ascher, P., and L. Nowak. The role of divalent cations in the NMDA responses of mouse central neurones in culture. *J. Physiol. (Lond.)* **399**:247–266 (1988).
15. Wright, J. M., P. A. Kline, and L. M. Nowak. Multiple effects of tetraethyl-

ammonium on *N*-methyl-D-aspartate receptor-channels in cultured mouse brain neurons in cell culture. *J. Physiol. (Lond.)* **439**:579–604 (1991).
16. Colquhoun, D., and F. J. Sigworth. Fitting and statistical analysis of single-channel records, in *Single-Channel Recording* (B. Sakmann and E. Neher, eds.). Plenum Press, New York, 191–263 (1983).
17. Johnson, J. W., and P. Ascher. Glycine potentiates the NMDA response in cultured mouse brain neurons. *Nature (Lond.)* **325**:529–531 (1987).
18. Kleckner, N. W., and R. Dingledine. Requirement for glycine in activation of NMDA-receptors expressed in *Xenopus* oocytes. *Science (Washington, D. C.)* **241**:835–837 (1988).
19. Adams, P. R. Drug blockade of open end-plate channels. *J. Physiol. (Lond.)* **260**:531–553 (1976).
20. Neher, E., and J. H. Steinbach. Local anesthetics transiently block currents through single acetylcholine-receptor channels. *J. Physiol. (Lond.)* **277**:153–176 (1978).
21. Neher, E. The charge carried by single-channel currents of rat cultured muscle cells in the presence of local anesthetics. *J. Physiol. (Lond.)* **339**:663–678 (1983).
22. Rang, H. P. Drugs and ionic channels: mechanisms and implications. *Postgrad. Med. J.* **57**:89–97 (1981).
23. Pennefather, P., and D. M. J. Quastel. Modification of dose-response curves by effector blockade and uncompetitive antagonism. *Mol. Pharmacol.* **22**:369–380 (1982).
24. Ogden, D. C., S. A. Seigelbaum, and D. Colquhoun. Block of acetylcholine-activated ion channels by an uncharged local anesthetic. *Nature (Lond.)* **289**:596–598 (1981).
25. Hille, B. Local anesthetics: hydrophilic and hydrophobic pathways for the drug-receptor reaction. *J. Gen. Physiol.* **69**:497–515 (1977).
26. MacDonald, J. F., and L. M. Nowak. Mechanisms of blockade of excitatory amino acid receptor channels. *Trends Pharmacol. Sci.* **11**:167–172 (1990).

Send reprint requests to: Linda M. Nowak, Department of Pharmacology, Cornell University, College of Veterinary Medicine, Ithaca, NY 14853–6401.